Optimized Imploding Waves in the Coherent Control of Bimolecular Processes: Atom−Rotor Scattering

Einat Frishman and Moshe Shapiro*

Chemical Physics Department, The Weizmann Institute of Science, Rehovot, Israel

Paul Brumer

Photonics Research Ontario and Chemical Physics Theory Group, University of Toronto, Toronto, Canada M5S 3H6

Received: July 2, 1999; In Final Form: September 3, 1999

Sculpting the incoming wave in bimolecular scattering by varying its partial wave content is shown to provide an effective means of controlling the cross sections for bimolecular collisions. Applications to Ar + H_2 and Ar + HD, treated as atom−rigid rotor scattering, show enhancement factors of the outgoing flux for a selected rotational transition of more than an order of magnitude.

1. Introduction

Considerable work, over the past three decades, has gone into the study of atom−molecule inelastic collisions, including the development of extensive formalism and the calculation of cross sections for rotational, vibrational, and electronic excitations. All of these studies are designed to analyze the natural outcome of the inelastic scattering of atoms and molecules. By contrast, current interest lies in the ability to *control* the outcome of atomic and molecular processes. In particular, modern efforts in coherent control[1−12] have aimed at using lasers to introduce controllable quantum interference terms into the cross sections of atomic and molecular processes. As a consequence, varying specific laser parameters induce changes in these quantum interference terms which, in turn, significantly alter the natural yields and cross sections. Both detailed[1] and elementary[2] reviews of this coherent control approach are available.

Examining the coherent-control literature shows that the vast majority of controlled processes previously considered are unimolecular in nature, e.g., the photodissociation or photoionization of isolated molecules. Only recently have we shown[3−6] that the essential principle of coherent control can be used effectively to alter cross sections for scattering processes. That is, we demonstrated that if one collides two molecules in a superposition of *energetically degenerate* scattering states, then the resultant scattering cross section contains controllable interference terms.

For a general bimolecular collision of the type

$$A + BC(v,j) \rightarrow A' + B'C'(v'j')$$

where v and j are vibrational and rotational quantum numbers, the requirement that the total energy be the same means that we must choose all the interfering paths contributing to the process so that they are at energy

$$E = \epsilon_{v,j} + \hbar^2k^2/2\mu = \epsilon_{v'j'} + \hbar^2k'^2/2\mu \qquad (1)$$

Here $\epsilon_{v,j}$ denotes the internal state of the BC molecule with vibrational quantum number v and rotational quantum number j, and $\hbar^2k^2/2\mu$ is the $A-BC$ relative kinetic energy. Similar definitions hold for the primed symbols. Thus, if we attempt bimolecular control by colliding an initial superposition state Φ made up of, for example, two vib−rotational states,

$$\Phi = c_1|v_1,j_1\rangle + c_2|v_2,j_2\rangle \qquad (2)$$

then we must simultaneously correlate each component of the superposition state with a translational wavefunction whose **k** wave-vector satisfies eq 1, that is

$$\hbar^2k^2_{v_1j_1}/2\mu = E - \epsilon_{v_1j_1}, \quad \hbar^2k^2_{v_2j_2}/2\mu = E - \epsilon_{v_2j_2} \qquad (3)$$

That is, we must construct wavefunctions of the form

$$\Phi = c_1|v_1,j_1\rangle|\mathbf{k}_{v_1j_1}\rangle + c_2|v_2,j_2\rangle|\mathbf{k}_{v_2j_2}\rangle \qquad (4)$$

which satisfy eq 3. When $\epsilon_{v_1j_1} \neq \epsilon_{v_2j_2}$ this is not an easy task to achieve experimentally, although we have provided some suggested scenarios.[3,6] If, however, the internal states used in the initial superposition state Φ are degenerate, the condition (eq 3) on the relative momenta can be achieved automatically with a single translational energy.

In ref 4 we followed the latter approach by considering an initial superposition state comprised of degenerate m_j magnetic sublevels. The resultant scenario, while allowing control over the angular differential cross section, did not allow for control over the integral cross section. In this paper, we explore the possibility of using another combination of degenerate asymptotic states, that is, different orbital angular momentum partial waves l. In doing so, we deviate from the normal scattering experiment in which two plane waves representing two molecular beams are allowed to collide. Instead, by controlling the l components of the incoming wave, we create a *sculpted imploding wave* and explore its effect on specific quantum transitions.

Although this approach is applicable to any bimolecular collision, we apply it here to rotational excitation (and de-excitation), obtaining optimally constructed imploding waves.

* To whom correspondence should be addressed.

10.1021/jp9922920 CCC: $18.00
Published on Web 11/17/1999

We show that sculpting the incoming wave can lead to a considerable enhancement of integral cross sections for specific transitions.

The structure of this paper is as follows. In section 2, we summarize the usual theory of rotational excitation by collisions using plane wave beams of structureless atoms and rigid molecular rotors. In section 3, we develop the theory of scattering, and in particular rotational excitation, for the collision between two nonspherical imploding waves. In section 4, we show how to maximize the scattered flux associated with a specific transition by sculpting such nonspherical imploding waves. Finally, in section 5 we demonstrate the utility of our approach via two sample rotational excitation cases, the collision of an Ar atom with H_2 and with HD.

2. Rotational Inelastic Transitions with Incoming Plane-Waves

Here, we summarize the theory of rotational transitions for ordinary inelastic collisions, as formulated by Arthurs and Dalgarno.[13,14] Our purpose is not to repeat this well-know theory, but rather to establish the notation used in this paper and to emphasize the differences between a process occurring with ordinary plane-waves and with sculptured imploding waves.

Consider, then, an atomic projectile colliding with a rigid-rotor target whose coordinates are specified by two angles, θ and ϕ, which comprise the unit vector $\hat{r} = (\theta, \phi)$. The coordinates of the projectile relative to the rotor center of mass are denoted $R \equiv (R, \hat{R})$, with $\hat{R} \equiv (\Theta, \Phi)$ being a unit direction-vector. With the target Hamiltonian written as

$$H_{rot} = \frac{\hbar^2}{2I} j(j+1) \tag{5}$$

where I is the rotor's moment of inertia and j is the rotor's (internal) angular momentum operator, the total Hamiltonian is given as

$$H = H_{rot} - \frac{\hbar^2}{2\mu}\nabla^2_R + V(R, R\cdot\hat{r}) \tag{6}$$

Here, μ is the reduced mass of the atom-rotor system and $V(R,R\cdot\hat{r})$ is the atom−rotor interaction potential. It is convenient to introduce the functions $\Psi^{JM}_{jl}(R, \hat{r})$, which are the common eigenfunctions of H; the total angular momentum, J; and its projection on a space-fixed Z-axis, M, having entrance-channel internal and orbital angular momenta quantum numbers j and l, respectively. These functions satisfy the Schrödinger equation:

$$H\Psi^{JM}_{jl}(R, \hat{r}) = E\Psi^{JM}_{jl}(R, \hat{r}) \tag{7}$$

The total energy, E, is comprised of translational and internal rotational energies:

$$E = \frac{k_j^2}{2\mu} + \frac{\hbar^2}{2I} j(j+1) \tag{8}$$

with k_j being the channel wavenumber, given by eq 8 as

$$k_j^2 = \frac{2\mu}{\hbar^2}\left[E - \frac{\hbar^2}{2I} j(j+1)\right] \tag{9}$$

The Schrödinger equation can be solved[13] by expanding $\Psi^{JM}_{jl}(R, \hat{r})$ in bispherical harmonics:

$$\Psi^{JM}_{jl}(R, \hat{r}) = \sum_{j',l'} \frac{1}{R} u^J_{j'l'\leftarrow jl}(R)\, y^{JM}_{j'l'}(\hat{R}, \hat{r}) \tag{10}$$

where $y^{JM}_{jl}(\hat{R}, \hat{r})$, the bispherical harmonics, are defined as

$$y^{JM}_{jl}(\hat{R}, \hat{r}) = \sum_{m_l=-l}^{l} \sum_{m_j=-j}^{j} (jlm_jm_l; JM) Y_{lm_l}(\hat{R}) Y_{jm_j}(\hat{r}) \tag{11}$$

and are eigenfunctions of J, M, j, and l. Substituting eqs 5, 6, and 10 into eq 7 we obtain a set of coupled channel equations for the radial expansion coefficients $u^J_{j'l'\leftarrow jl}(R)$:

$$\frac{\hbar^2}{2\mu}\left[-\frac{d^2}{dR^2} + \frac{l'(l'+1)}{R^2} - k^2_{j'}\right] u^J_{j'l'\leftarrow jl}(R) + \sum_{j''}\sum_{l''} V^J_{j'l',j''l''}(R) u^J_{j''l''\leftarrow jl}(R) = 0 \tag{12}$$

where

$$V^J_{j''l'',j'l'}(R) \equiv \int\int y^{JM}_{j''l''}(\hat{R}, \hat{r}) V(R, \hat{r}) y^{JM}_{j'l'}(\hat{R}, \hat{r})\, d\hat{R}\, d\hat{r} \tag{13}$$

Equations 12 are solved numerically, subject to the boundary conditions,

$$u^J_{j'l'\leftarrow jl}(0) = 0,$$

$$\lim_{R\to\infty} u^J_{j'l'\leftarrow jl}(R) \sim -2i\delta_{jj'}\delta_{ll'} \sin(k_jR - l\pi/2) + \left(\frac{k_j}{k_{j'}}\right)^{1/2} T^J_{j'l'\leftarrow jl} e^{+i(k_{j'}R - l'\pi/2)} = \delta_{jj'}\delta_{ll'} e^{-i(k_jR - l\pi/2)} - \left(\frac{k_j}{k_{j'}}\right)^{1/2} S^J_{j'l'\leftarrow jl} e^{+i(k_{j'}R - l'\pi/2)} \tag{14}$$

where $S^J_{j'l'\leftarrow jl}$, an element of the S matrix, is given in terms of $T^J_{j'l'\leftarrow jl}$ of eq 14 as

$$S^J_{j'l'\leftarrow jl} = \delta_{jj'}\delta_{ll'} - T^J_{j'l'\leftarrow jl} \tag{15}$$

The asymptotic behavior of the wavefunction can be written as

$$\lim_{R\to\infty} \Psi^{JM}_{jl}(R, \hat{r}) = \Psi^{in}(R, \hat{r}) + \Psi^{sc}(R, \hat{r}) \tag{16}$$

where the second term represents a scattered wave, and the first term represents either a plane-wave (whose partial wave components are given in the second line of eq 14) or an *imploding spherical wave* (with partial wave components given in the last time of eq 14).

Given the S matrix, the probability of observing a rotational transition from state jl to state $j'l'$ for fixed J is given as

$$P^J_{j'l'\leftarrow jl} = |S^J_{j'l'\leftarrow jl}|^2 \tag{17}$$

3. Scattering of Sculpted Imploding Waves

We now generalize the treatment of section 2 to include a collision with nonspherical imploding waves. Use of such imploding waves offers a powerful method to control the outcome of the collision and to alter the rotational transition probabilities.

Nonspherical imploding waves are formally obtained by considering superpositions of $\Psi_{jl}^{JM}(R, \hat{r})$ with arbitrary complex coefficients $\{c_{jl}^{JM}\}$

$$\psi_j(R, \hat{r}) = \frac{i}{k_j} \sum_{J=0}^{\infty} \sum_{M=-J}^{J} \sum_{l=|J-j|}^{J+j} c_{jl}^{JM} \Psi_{jl}^{JM}(R, \hat{r}) \tag{18}$$

However, since our interest is control via changes in m_j and m_l rather than J and M, it is more convenient to specify the superposition state via m_j- and m_l-dependent coefficients, denoted as $d_{jl}^{m_j m_l}$, which are related to the c_{jl}^{JM} coefficients by a unitary transformation of the form

$$c_{jl}^{JM} = \sum_{m_j=-j}^{j} \sum_{m_l=-l}^{l} (jlm_jm_l; JM)\, d_{jl}^{m_j m_l} \tag{19}$$

Comparing eqs 19 and 18 with eq 10, we see that for an incoming plane-wave, $d_{jl}^{m_j m_l}(plane) = i^l\sqrt{\pi}\sqrt{2l+1}\delta_{m_j m^0}\delta_{m_l 0}$ where m^0 is the specification for the initial j projection.

By analogy to eq 16, we can break the asymptotic expansion of ψ_j into incoming and scattered parts:

$$\lim_{R\to\infty} \psi_j(R, \hat{r}) = \psi_j^{in}(R, \hat{r}) + \psi_j^{sc}(R, \hat{r}) \tag{20}$$

where

$$\psi_j^{in}(R, \hat{r}) = 2\sum_{JMl} c_{jl}^{JM} j_l(k_j R) y_{jl}^{JM}(R, \hat{r}) \tag{21}$$

and

$$\psi_j^{sc}(R, \hat{r}) = \frac{i}{k_j R} \sum_{JMl} c_{jl}^{JM} \sum_{j'l'} \left(\frac{k_j}{k_{j'}}\right)^{1/2} T_{j'l'\leftarrow jl}^{J} e^{+i(k_{j'}r - l'\pi/2)} y_{j'l'}^{JM}(\hat{R}, \hat{r}) \tag{22}$$

Substituting eqs 11 and 19 in eq 21 and using the orthogonality property of the Clebsch-Gordan coefficients[15] allows us to express the incoming wavefunction in terms of $\{d_{jl}^{m_j m_l}\}$ as

$$\psi_j^{in}(R, \hat{r}) = 2\sum_{l} \sum_{m_j m_l} d_{jl}^{m_j m_l} j_l(k_j R)\, Y_{lm_l}(\hat{R}) Y_{jm_j}(\hat{r}) \tag{23}$$

For cylindrically symmetric potentials, the k_j vector can be chosen in the z direction, and the summation over m_l reduces to the single term $m_l = 0$. As a result, $\psi_j^{in}(R, \hat{r})$ depends on the angle θ between k_j and R but is independent of the azimuthal angle ϕ.

Defining a *generalized* scattering amplitude as

$$f_{j'm_{j'}\leftarrow jm_j}(\hat{R}) = \sum_{lm_l} d^{m_j m_l}{}_{jl} \sum_{l'm_{l'}} i^{-l'} Y_{l'm_{l'}}(\hat{R}) \sum_{JM} (jlm_jm_l; JM) \times (j'l'm_{j'}m_{l'}; JM) T_{j'l'\leftarrow jl}^{J} \tag{24}$$

we can write $\psi_j^{sc}(R, \hat{r})$ as

$$\psi_j^{sc}(R,\hat{r}) = \frac{i}{k_j R} \sum_{j'm_{j'}} \sum_{m_j} f_{j'm_{j'}\leftarrow jm_j}(\hat{R}) \left(\frac{k_j}{k_{j'}}\right)^{1/2} e^{+ikj'R} Y_{j'm_{j'}}(\hat{r}) \tag{25}$$

We now proceed to derive expressions for the incoming and scattered fluxes associated with a general incoming wave. We concentrate on fluxes, rather than cross sections, for the following reason. Plane-waves have a uniform incoming flux coming from *a single* direction and allow for the definition of a cross section as the ratio between the scattered flux and the incoming flux per unit area. However, an arbitrary incoming wave has multidirectional and nonspherical incoming and scattered fluxes. Hence the term "incoming flux per unit area" is meaningless, and a cross section cannot be defined. We therefore adopt the strategy of working separately with the incoming (or imploding) and scattered fluxes and show below (see section 4) how to choose the $\{d_{jl}^{m_j m_l}\}$ coefficients to maximize the scattered flux into a given rotor state j'.

The imploding part of the wavefunction in the $R \to \infty$ limit:

$$\psi^{imp}{}_j(R, \hat{r}) \sim \frac{-2e^{-ik_j R}}{ik_j R} \sum_{l} \sum_{m_j m_l} i^l d_{jl}^{m_j m_l} Y_{lm_l}(\hat{R}) Y_{jm_j}(\hat{r}) \tag{26}$$

has an associated flux

$$F_j^{imp}(R, \hat{r}) = -\frac{i\hbar}{2\mu}\left[\psi_j^{imp*}(R, \hat{r}) \frac{\partial \psi_j^{imp}(R, \hat{r})}{\partial R} - \psi_j^{imp}(R, \hat{r}) \frac{\partial \psi_j^{imp*}(R, \hat{r})}{\partial R}\right] \hat{n} \tag{27}$$

where $\hat{n}$ is a radial unit vector. Using the fact that as $R \to \infty$, $\partial\psi_j^{imp}(R,\hat{r})/\partial R \sim -ik_j\psi_j^{imp}(R, \hat{r})$, we integrate $F_j^{imp}(R, \hat{r})$ over $\hat{R}$ (at radius R) and over $\hat{r}$ to obtain the total flux of $\psi_j^{imp}(R, \hat{r})$ entering a sphere of radius R:

$$F_j^{imp} = \frac{\hbar}{\mu} \mathrm{Im}\left[R^2 \int\int d\hat{r}\, d\hat{R}\, \psi_j^{imp*}(R, \hat{r}) \frac{\partial \psi_j^{imp}(R, \hat{r})}{\partial R}\right] = -\frac{\hbar k_j}{\mu} R^2 \int\int d\hat{r}\, d\hat{R} |\psi_j^{imp}(R, \hat{r})|^2 = -\frac{4\hbar}{\mu k_j} \sum_{l} \sum_{m_j m_l} |d_{jl}^{m_j m_l}|^2 \tag{28}$$

We see that the imploding flux is proportional to the total population of all $\{l, m_l, m_j\}$-states in the incoming wave. Any unitary transformation on $d_{jl}^{m_j m_l}$ conserves this quantity.

For a plane-wave, $d_{jl}^{mjml}(plane) = i^l\sqrt{\pi}2l + 21\delta_{m_j m^0}\delta_{m_l 0}$. Therefore,

$$\sum_{l} \sum_{m_j m_l} |d^{m_j m_l}_{jl}(plane)|^2 = \pi \sum_{l} (2l + 1) \tag{29}$$

This sum, and hence F_j^{imp} for the plane-wave, are infinite. In order to be able to compare the effectiveness of rotational transitions using a general imploding wave to that of a plane-wave, we consider only a finite portion of both waves by introducing a cutoff angular momentum l_f, chosen to be the highest angular momentum which contributes effectively to the scattering process.

Using a similar calculation as for $\psi_j^{imp}(R, \hat{r})$, the scattered flux of $\psi_j^{sc}(R, \hat{r})$ into j', m_j' is given by

$$F_{j'm_{j'}\leftarrow j,m_j}^{scat} = \frac{\hbar}{\mu k_j} \int d\hat{R} |f_{j'm_{j'}\leftarrow jm_j}(\hat{R})|^2 \tag{30}$$

Related, m_j- and/or $m_{j'}$-summed fluxes are given as

$$F_{j'm_{j'}\leftarrow j}^{scat} = \sum_{m_j} F_{j'm_{j'}\leftarrow j,m_j}^{scat};\ F_{j'\leftarrow j,m_j}^{scat} = \sum_{m_{j'}} F_{j'm_{j'}\leftarrow j,m_j}^{scat};\ F_{j'\leftarrow j}^{scat} = \sum_{m_j,m_{j'}} F_{j'm_{j'}\leftarrow j,m_j}^{scat} \tag{31}$$

After some algebra, it is possible to show that

$$F^{scat}_{j'm_{j'}\leftarrow j} = \frac{\hbar}{\mu k_j}\sum_{l'm_{l'}}\left|\sum_{JMl} c^{JM}_{jl}(j'l'm_{j'}m_{l'};\, JM)T^{J}_{j'l'\leftarrow jl}\right|^2 \qquad (32)$$

[if $j = j'$, $m_j = m_{j'}$, an additional (infinite) scattered flux exists from the *incoming* wavefunction $\psi^{in}_j(\mathrm{R}, \hat{\mathrm{r}})$] and that

$$F^{scat}_{j'\leftarrow j,m_j} = \frac{\hbar}{\mu k_j}\sum_{JMl'}\left|\sum_{lm_l} d^{m_jm_l}_{jl}(jlm_jm_l;\, JM)T^{J}_{j'l'\leftarrow jl}\right|^2 \qquad (33)$$

In a similar fashion we can show that

$$F^{scat}_{j'\leftarrow j} = \frac{\hbar}{\mu k_j}\sum_{JMl'l''} c^{JM}_{jl}\, c^{*JM}_{jl''}\, T^{J}_{j'l'\leftarrow jl}\, T^{*J}_{j'l'\leftarrow jl''}\,\delta(j'l'J) = \frac{\hbar}{\mu k_j}\sum_{JMl'}\left|\sum_{l} c^{JM}_{jl}\, T^{J}_{j'l'\leftarrow jl}\right|^2 \qquad (34)$$

4. Maximization of the Scattered Flux

Consider now maximizing the scattered flux into a given j' state, subject to various constraints. The control parameters are the $d^{m_jm_l}_{jl}$ coefficients, which shape the input wavefunction $\psi^{in}_j(\mathrm{R}, \hat{\mathrm{r}})$. Our strategy is to formulate the problem as a linear optimization problem in these coefficients.

Note first that if we average on m_j, then control is possible only if the $d^{m_jm_l}_{jl}$ coefficients depend upon m_j. That is, if $d^{m_jm_l}_{jl}$ are independent of m_j, that is, if $d^{m_jm_l}_{jl} = d^{m_l}_{jl}$, then no phase control over the rotational transitions is possible. In order to see this, consider the nonpolarized flux, given (in the absence of m_j dependence), by

$$F^{scat}_{j'\leftarrow j} = \frac{\hbar}{\mu k_j}\frac{1}{(2j+1)}\sum_{lm_l}\sum_{l'm_{l'}} d^{m_l}_{jl}\, d^{*m_{l'}}_{jl''}\sum_{JMmjl'}(jlm_jm_l;\, JM)\times (jl''m_jm_{l'};\, JM)T^{J}_{j'l'\leftarrow jl}\, T^{*J}_{j'l'\leftarrow jl''} \qquad (35)$$

Using the orthogonality of the Clebsch-Gordan coefficients,[15] we obtain

$$F^{scat}_{j'\leftarrow j} = \frac{\hbar}{\mu k_j}\frac{1}{(2j+1)}\sum_{Jl'}\sum_{lm_{l'}}\left(\frac{2J+1}{2l+1}\right)|d^{m_l}_{jl}|^2|T^{J}_{j'l'\leftarrow jl}|^2 \qquad (36)$$

That is, the flux no longer depends upon the phase of the $d^{m_jm_l}_{jl}$ coefficients. This loss of control by incoherent averaging over m_j is reminiscent of similar results obtained for m_j control over collision processes.[4]

Consider next maximizing the scattered flux to a given j' manifold for an incoming wave comprised of only one m_j state. For this case we have, using eq 33,

$$F^{scat}_{j'\leftarrow j,m_j} = \frac{\hbar}{\mu k_j}\sum_{ll''}\sum_{m_lm_{l''}} d^{m_jm_l}_{jl}\, d^{*m_lm_{l''}}_{jl''}\, B^{jj'm_j}_{l''lm_{l''}m_l} \qquad (37)$$

where

$$B^{jj'm_j}_{l''lm_{l''}m_l} \equiv \sum_{JMl'}(jlm_jm_l;\, JM)(jl''m_jm_{l'};\, JM)T^{J}_{j'l'\leftarrow jl}\, T^{*J}_{j'l'\leftarrow jl''} \qquad (38)$$

It is easy to show that the $B^{jj'm_j}$ matrices are Hermitian.

Two strategies for control over F^{scat} are in principle possible: the first is "classical", in which we essentially choose favorable values of l and m_l, for which the $B^{jj'm_j}$ matrix elements are largest. The other is quantum mechanical: we allow interference between all the amplitudes comprising the incoming wave. The latter is more general and is utilized here.

Within the framework of the quantum strategies, it is possible to optimize the $d^{m_jm_l}_{jl}$ coefficients, subject to the constraint that either the total incoming flux is the same as that of a plane wave or that the normalization of the incoming wavefunction is the same as that of a plane wave:

$$\int \mathrm{dR}\mathrm{d}\hat{\mathrm{r}}\,\psi^{*in(1)}_{j1}(\mathrm{R},\hat{\mathrm{r}})\psi^{in(2)}_{j2}(\mathrm{R},\hat{\mathrm{r}}) = \delta_{j1j2}\delta(k^{(1)}_{j1} - k^{(2)}_{j2}) \qquad (39)$$

Both constraints are considered below. In particular, details of the constraints are discussed in section 4.1 and 4.2, and results are presented in section 5.

4.1. Optimization Subject to Incoming Flux Constraint. In order to equate the incoming flux, given in eq 28 with its plane-wave value, we introduce a Lagrange multiplier $\lambda_{j'}$:

$$F^{\lambda}_{j'\leftarrow j,m_j} = \frac{\hbar}{\mu k_j}\left[\sum_{lm_l}\sum_{l''m_{l''}} d^{m_jm_l}_{jl}\, d^{*m_jm_{l''}}_{jl''}\, B'^{ijm_j}_{l''lm_{l''}m_l} - \lambda_{j'}\sum_{lm_l}(|d^{m_jm_l}_{jl}|^2 - |d^{m_jm_l}_{jl}(plane)|^2)\right] \qquad (40)$$

Differentiating with respect to $d'^{*m_jm_{l'}}_{jl''}$ to obtain the extremum points of $F^{\lambda}_{j'\leftarrow j,m_j}$, we obtain the condition

$$\sum_{m_l}\sum_{l} d^{m_jm_l}_{jl}\, B^{jj'm_j}_{l''lm_{l''}m_l} = \lambda_{j'} d^{m_jm_{l''}}_{jl''} \qquad l'' = 0, 1, \ldots \qquad (41)$$

Defining a $\mathrm{d}_{j,m_j} \equiv \{d^{m_jm_l}_{jl}\}$ eigenvector, whose dimension is the number of possible initial l-states, we can write eq 41 in matrix form as

$$\mathrm{B}^{jj'm_j}\cdot\mathrm{d}_{j,m_j} = \mathrm{d}_{j,mj}\cdot\lambda_{j'} \qquad (42)$$

where $\lambda_{j'}$ is a diagonal matrix of eigenvalues.

The flux associated with each eigenvector is proportional to the value of the corresponding eigenvalue $\lambda_{j'}$, since by eqs 40 and 42

$$F^{\lambda}_{j'\leftarrow j,m_j} = \frac{\hbar}{\mu k_j}\left[\mathrm{d}^{\dagger}_{j,m_j}\cdot\mathrm{B}^{jj'm_j}\cdot\mathrm{d}_{j,m_j} - \lambda_{j'}\left(\mathrm{d}^{\dagger}_{j,m_j}\cdot\mathrm{d}_{j,m_j} - \mathrm{d}^{\dagger}(plane)\cdot\mathrm{d}(plane)\right)\right]$$
$$= \frac{\hbar}{\mu k_j}\left[\lambda_{j'}\mathrm{d}^{\dagger}(plane)\cdot\mathrm{d}(plane)\right] = \frac{\hbar}{\mu k_j}\pi\lambda_{j'}\sum_{l=0}^{l_f}(2l+1) = \frac{\hbar}{\mu k_j}\pi\lambda_{j'}(l_f+1)^2 \qquad (43)$$

Thus, the scattered flux associated with the $j' \leftarrow j$, m_j transition is $\lambda_{j'}$ times the l_f-truncated sum of the partial-waves weights associated with an incoming plane-wave. In particular, the maximal eigenvalue yields the maximal flux. Since the optimal $\lambda_{j'}$ for one $j' \leftarrow j$ transition will not necessarily enhance the flux associated with any other transition, this control scenario provides a great degree of selectivity of one rotational transition over another.

4.1.1. The Cutoff Angular Momentum l_f. For a plane wave, $F^{scat}_{j'\leftarrow j,m_j} = (\hbar/\mu k_j)\mathrm{d}^{\dagger}(plane)\cdot\mathrm{B}\cdot\mathrm{d}(plane)$. For high l's, $|B^{jj'm_j}_{l''lm_{l'}m_l}| \rightarrow 0$ faster than $1/(d^{m_jm_l}_{jl}\, d'^{*m_jm_{l'}}_{jl'})$, and therefore F^{scat} is finite, even if $\mathrm{d}^{\dagger}\mathrm{d}$ is infinite. By contrast, according to eq 43, the optimal solution does not contain $|B^{jj'm_j}_{l''lm_{l'}m_l}|$, and $F^{\lambda}_{j'\leftarrow j,m_j}$ is only

limited by the choice of l_f. As we increase l_f in the construction of the optimal imploding wave we can achieve larger and larger scattered flux into the target j' manifold. Nonetheless, choosing l_f arbitrarily large may not be the best practical approach to increasing the cross section, since the difficulty of preparing the imploding wave in the laboratory is expected to increase with increasing l_f.

In order to decide what type of optimization problem we want to solve, we choose the cutoff parameter l_f according to the following procedure: we calculate the diagonal contribution $(\hbar/\mu k_j)\pi(2l+1)B^{jj'0}_{l'l00}$ of the l-components of a plane-wave (for $m_j = 0$) to the scattered flux (see eq 37) and truncate the sum when this value dips below a preset fraction (1%) of its maximal value.

We emphasize again that for a nonuniform imploding wave, each choice of l_f corresponds to a different scattered flux and hence to a different optimization problem. The above choice of l_f corresponds to optimizing the imploding wave for the first l_f partial wave and setting the weights of the remaining $l > l_f$ partial waves to the values for a plane-wave. These partial waves no longer contribute to the inelastic process of interest.

4.2. Optimization Subject to Incoming Wavefunction Normalization Constraint. If we require the incoming wavefunction $\psi_j^{in}(\mathrm{R}, \hat{\mathrm{r}})$ to satisfy a $\delta_{j_1 j_2}\delta(k_{j_1}^{(1)} - k_{j_2}^{(2)})$ normalization condition (eq 39), the coefficients which make up the imploding wave must satisfy (see Appendix) the constraint

$$\sum_{m_j} d_{j_1 l}^{*m_j m_{l1}}\, d_{j_1 l}^{m_j m_{l2}} = \pi(2l+1)\delta_{m_{l1}0}\delta_{m_{l2}0} \tag{44}$$

for every l, m_{l_1}, and m_{l_2}.

In the cylindrically symmetric case $m_l = 0$, and if we consider one m_j value, then

$$d_{jl}^{m_j 0} = i^l\sqrt{\pi}\sqrt{2l+1}\,\mathrm{e}^{i\theta_{jl}^{m_j 0}} \tag{45}$$

That is, the magnitude for each l component is the same as in the plane-wave, and the only free parameters that can be optimized are the phases $\{\theta_{jl}^{m_j 0}\}$. The scattered flux of $\psi_j^{sc}(\mathrm{R}, \hat{\mathrm{r}})$ is now given by

$$F^{scat}_{j'\leftarrow j,m_j} = \frac{\hbar}{\mu k_j}\sum_{ll''}\pi(2l+1)^{1/2} (2l''+1)^{1/2} i^{l-1''}\,\mathrm{e}^{i(\theta_{jl}^{m_j 0} - \theta_{j'}^{m_j 0})}\, B^{ij'm_j}_{l''lm_l''m_l} \tag{46}$$

The optimization is performed by a nonlinear search routine in the $\{\theta_{jl}^{m_j 0}\}$ space of phases.

5. Computational Results

5.1. The Model. To demonstrate the possible control afforded by sculpting the imploding wave, we consider a rotational excitation problem, studied in refs 16 and 17, and compare the imploding wave results to those obtained with plane waves. Following refs 16 and 17, we expand $V(R, \hat{\mathrm{R}}\cdot\hat{\mathrm{r}})$, the projectile−rotor interaction potential, in a series of Legendre polynomials[18] and truncate the expansion, as appropriate for a weakly anisotropic system, after the first three terms:

$$V(R, \hat{\mathrm{R}}\cdot\hat{\mathrm{r}}) = V_0(R) + V_1(R)P_1(\hat{\mathrm{R}}\cdot\hat{\mathrm{r}}) + V_2(R)P_2(\hat{\mathrm{R}}\cdot\hat{\mathrm{r}}) \tag{47}$$

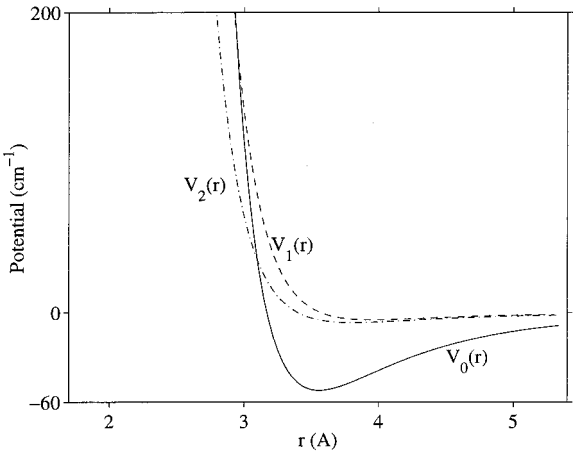

Figure 1. Isotropic potential $V_0(R)$ and leading anisotropic potentials for the Ar−HD and Ar−H_2 systems.

The terms $V_0(R)$ and $V_2(R)$ are parametrized by Lennard-Jones potentials:[19,20,22]

$$V_0(R) = \epsilon_0[(R_0^e/R)^{12} - 2(R_0^e/R)^6] \tag{48}$$

$$V_2(R) = \epsilon_2[(R_2^e/R)^{12} - 2(R_2^e/R)^6] = a_2\epsilon_0[q(R_0^e/R)^{12} - 2(R_0^e/R)^6] \tag{49}$$

where

$$q \equiv (R_2^e/R_0^e)^6 \quad \text{and} \quad a_2 \equiv (\epsilon_2/\epsilon_0)q$$

For a heteronuclear diatom composed of two isotopes (such as HD), we can compute $V_1(R)$ as[23]

$$V_1(R) = -\delta\left[\frac{dV_0(R)}{dR} + 0.4\frac{dV_2(R)}{dR} + \frac{1.2}{R}V_2(R)\right]$$

where δ is the displacement of the center of mass of the diatom from the center of force. The potentials $V_0(R)$, $V_1(R)$ (for Ar−HD), and $V_2(R)$ are shown in Figure 1.

By defining a dimensionless variable $x \equiv R/R_m$ and a dimensionless potential $V^* = V/\epsilon$, where $R_m = R_0^e$ and $\epsilon = \epsilon_0$, the Coupled Channels equations (eq 12) assume the form

$$\left[-\frac{\mathrm{d}^2}{\mathrm{d}x^2} + \frac{l'(l'+1)}{x^2} - K_{j'}^2\right]u^J_{j'l'\leftarrow jl}(x) + B\sum_{j''}\sum_{l''}V^J_{j'l',j''l''}(x)u^J_{j''l''\leftarrow jl}(x) = 0 \tag{50}$$

where

$$B = \frac{2\mu\epsilon R_m^2}{\hbar^2} \quad \text{and} \quad K_j^2 = k_j^2 R_m^2 = \frac{2\mu R_m^2}{\hbar^2}\left[E - \frac{\hbar^2}{2I}j(j+1)\right] \tag{51}$$

The dynamics is seen to be determined by three dimensionless parameters: B, BE/ϵ, $\mu R_m^2/I$, and by the form of the potential chosen.

We consider the Ar−H_2 system as an example of a homonuclear molecule and the Ar−HD systems as an example of a heteronuclear molecule. The effect of δ on V_0 and on V_2 is of the order of δ^2 and is therefore ignored, and we take V_0 and V_2

TABLE 1: Scattered Flux Associated with All the $j' \leftarrow j = 2$, $m_j = 0$ Transitions when the $j' = 4$ State Is Optimized[a]

(a) Ar−HD System

j'	plane-wave	maximum (flux norm)	$\times 10^3/\pi(l_f+1)^2$	maximum (wfn norm)	minimum (wfn norm)
4	16.3	55.5	7.4	22.0	13.9
		Other Transitions			
0	6.2	0.6	0.1	5.8	15.0
1	37.9	19.8	2.6	49.8	18.0
2	137.2	43.9	5.8	112.9	148.5
3	38.2	31.4	4.2	45.0	40.4
5	2.0	12.8	1.7	2.3	2.0
6	0.1	0.1	0.0	0.1	0.1

(b) Ar−H_2 System

j'	plane-wave	maximum (flux norm)	$\times 10^3/\pi(l_f+1)^2$	maximum (wfn norm)	minimum (wfn norm)
4	1.6	7.4	1.7	2.0	1.0
		Other Transitions			
0	10.5	50.8	11.8	24.4	7.7
2	420.9	112.2	26.1	406.7	424.4

[a] All values have been multiplied by a factor of 1000.

TABLE 2: Scattered Flux Associated with All the $j' \leftarrow j = 2$, $m_j = 0$ Transitions when the $j' = 0$ State Is Optimized[a]

(a) Ar−HD System

j'	plane-wave	maximum (flux norm)	$\times 10^3/\pi(l_f+1)^2$	maximum (wfn norm)	minimum (wfn norm)
0	6.2	66.3	6.7	37.7	0.9
		Other Transitions			
1	37.9	38.4	3.9	33.2	47.3
2	137.2	34.4	3.5	117.4	124.2
3	38.2	54.7	5.5	32.0	44.5
4	16.3	20.2	2.1	15.0	18.9
5	2.0	0.4	0.0	2.1	2.0
6	0.1	0.0	0.0	0.5	0.1

(b) Ar−H_2 System

j'	plane-wave	maximum (flux norm)	$\times 10^3/\pi(l_f+1)^2$	maximum (wfn norm)	minimum (wfn norm)
0	10.5	92.4	13.3	34.8	0.6
		Other Transitions			
2	420.9	171.5	24.7	396.3	431.3
4	1.6	11.0	1.6	2.0	1.3

[a] All values have been multiplied by a factor of 1000.

to be the same for both Ar−H_2 and Ar−HD. For V_1, the leading term is proportional to δ, and the next term, neglected here, is proportional to δ^3.

The potential parameters chosen to model these systems are $\epsilon_0 = 52.21$ cm^{-1}, $R_0^e = 3.5573$ Å, $\epsilon_2 = 6.78$ cm^{-1}, $R_2^e = 3.814$ Å, δ(Ar−HD) = 0.1276 Å.[21,22] Therefore, $a_1 = 0.0359$, $a_2 = 0.198$, and $q = 1.52$. $\mu_{Ar-H_2} = 1.9188$ amu, $\mu_{Ar-HD} = 2.8099$ amu. The H_2 and HD rotational constants are $B_e = 60.80$ and 45.655 cm^{-1}, respectively.[24]

We obtain the $S^J_{j'l' \leftarrow jl}$ matrix elements by propagating the Coupled Channels equations [eq 50] using Gordon's method[25] until we reach the asymptotic region, where the appropriate boundary conditions [eq 14] are imposed. In this case, there are seven open channels ($j = 0, ..., 6$) for Ar−HD at $E_{tot} = 2000$ cm^{-1} and three open channels ($j = 0, 2, 4$) for Ar−H_2 at the same energy. Fixing j_{max}, the maximal j quantum number, to 6, results in (at most) 16 channels for each J. The calculation was repeated for each J value, whose maximal value is given as $J_{max} = j_{max} + l_f$.

The properties of the $\int\int y^{JM}_{j''l''}(\hat{R}, \hat{r})^*\, P_l(\hat{R}\cdot\hat{r})\, y^{JM}_{j'l'}(\hat{R},\hat{r})\, d\hat{R}\, d\hat{r}$ matrix elements[20] ensure that the $V_2(R)P_2(\hat{R}\cdot\hat{r})$ term can only couple j quantum number values of the same parity. The same holds for the l quantum numbers. Therefore, $B^{jj'm_j}_{l''lm_l'm_l}$ vanishes if either of $j - j'$ or $l'' - l$ are odd. This is also the case if there is a $V_1(R)$ potential, but $m_j = 0$ (due to the fact that one of the Clebsch-Gordon coefficients in eq 38 is zero). Hence, the $\mathbf{B}^{jj'}_{m_j i}$ matrix factors into an odd-l block and an even-l block, which are diagonalized separately. The overall maximal eigenvalue, therefore, corresponds to a d_{j,m_j} vector with only odd or only even components. The optimized wavefunction is therefore parity-adapted, $\psi_j(R, \hat{r}) = (-1)^p \psi_j(-R, \hat{r})$, where p is the parity of the l states in the expansion.

Below, we discuss the optimization results for four cases: the $j' = 4 \leftarrow j = 2$ and the $j' = 0 \leftarrow j = 2$ transitions for Ar colliding with HD and for Ar colliding with H_2, at a collision energy of $E = 2000$ cm^{-1}. We focus on the case of initial $m_j = 0$.

5.2. Optimization Constrained by the Incoming Flux. Tables 1 and 2 show, in column 3, the flux into all final j', having optimized the results for $j' = 4 \leftarrow j = 2$, $m_j = 0$ or $j' = 0 \leftarrow j = 2$, $m_j = 0$ for both Ar + H_2 and Ar + HD.

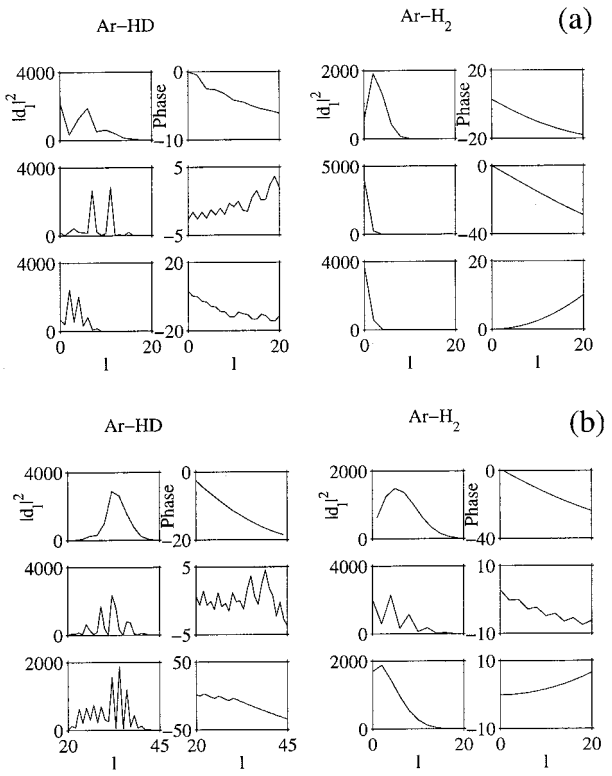

Figure 2. l-Components of the d_{j,m_j} eigenvector (left, absolute square; right, phase) leading to a maximal flux for the Ar−HD and Ar−H_2 systems: (a) $j' = 4 \leftarrow j = 2$, $m_j = 0, 1, 2$; (b) $j' = 0 \leftarrow j = 2$, $m_j = 0, 1, 2$; using the flux-normalization condition. For $m_j = 0$, only even or only odd l-values have nonzero d_l components; hence, only those are shown.

For example, the maximum flux for rotational excitation into $j' = 4$ for Ar + HD is 0.055, as compared to the partial wave result (column 2) of 0.016. Note also that the optimization into $j' = 4$, for example, does not necessarily decrease (or increase) the flux into $j' \neq 4$. That is, each optimization is selective to the particular product channel optimized.

The l-components of the eigenvector d_{j,m_j} leading to a maximal flux for the $j' = 4 \leftarrow j = 2$ and the $j' = 0 \leftarrow j = 2$ transitions are shown in Figure 2. Clearly, as can be seen, lower angular momenta contribute to the Ar−H_2 scattering than to Ar−HD.

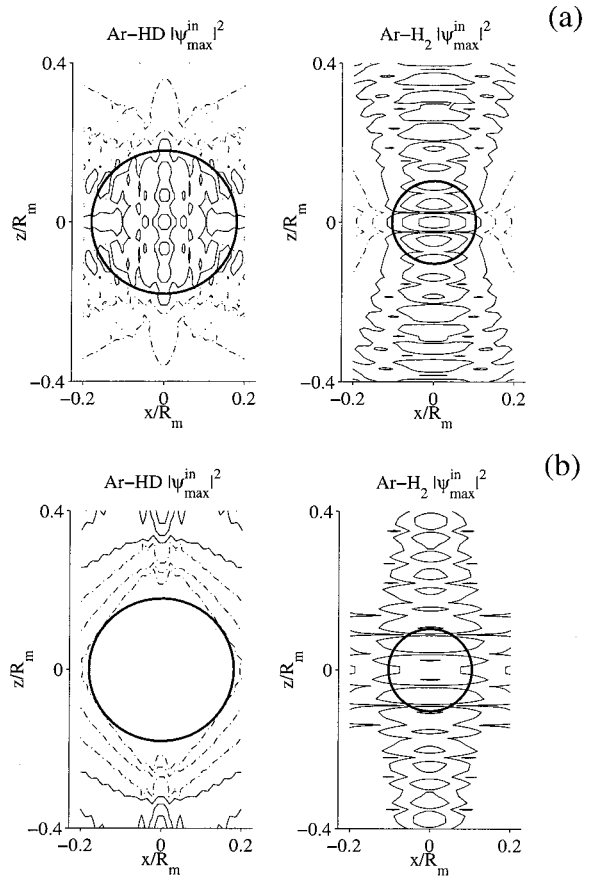

Figure 3. Square of the absolute value of the incoming wavefunction leading to maximum outgoing flux for the Ar−HD and Ar−H_2 systems using flux-normalization condition. The circle depicts the size of the diatomic: (a) $j' = 4 \leftarrow j = 2$, $m_j = 0$ optimization, maximum values of $|\psi^{in}_{max}|^2$ are 520 for Ar−HD and 163 for Ar−H_2; (b) $j' = 0 \leftarrow j = 2$, $m_j = 0$ optimization, maximum values of $|\psi^{in}_{max}|^2$ are 235 for Ar−HD and 125 for Ar−H_2. Solid line contours correspond to 0.5, 0.1, and 0.01 of the maximum value; dashed contours are for 10^{-3}, 10^{-4}, and 10^{-5} of the maximum.

Similarly, lower angular momenta contribute more to the optimized excitation process ($j' = 4 \leftarrow j = 2$) than to the optimized de-excitation ($j' = 0 \leftarrow j = 2$) process.

The cutoff values for the angular momentum are $l_f = 48$ and 36 for Ar−HD and Ar−H_2, respectively, for the $j' = 4 \leftarrow j = 2$, $m_j = 0$ case (Table 1) and 55 and 46 for the $j' = 0 \leftarrow j = 2$, $m_j = 0$ case (Table 2). In order to be able to compare those results, we also give the maximal flux divided by the normalization factor of $\pi(l_f + 1)^2$.

The absolute square value of the incoming wavefunction corresponding to the maximal flux are shown in Figure 3. These should be compared to an incoming plane-wave, whose absolute value is unity. Values for the maximal flux for these cases are provided in the figure captions, from which it is clear that the Ar + HD wavefunctions are less dispersed than those for Ar + H_2. Note that the incoming wavefunctions for the four cases shown in Figure 3 are remarkably different from one another in topology. For example, $|\psi^{in}_{max}|^2$ for Ar + HD $j' = 0 \leftarrow j = 2$ de-excitation is dominant at large values of *z*, whereas the Ar + HD $|\psi^{in}_{max}|^2$ for excitation $j' = 4 \leftarrow j' = 2$ is heavily concentrated at small *z*. A similar difference is not seen for the Ar + H_2 case.

The differential cross section is shown, for initial $m_j = 0$ values (summed over all final $m_{j'}$ values), in Figure 4. Interestingly, the optimized cross sections are symmetric about $\theta =$ 90°, whereas the plane-wave result tends to peak near $\theta = 180°$. This is because (for $m_j = 0$) only *l* values of the same parity contribute to the final result, a consequence of the fact that the ***B*** matrix does not couple *l* values of different parity.

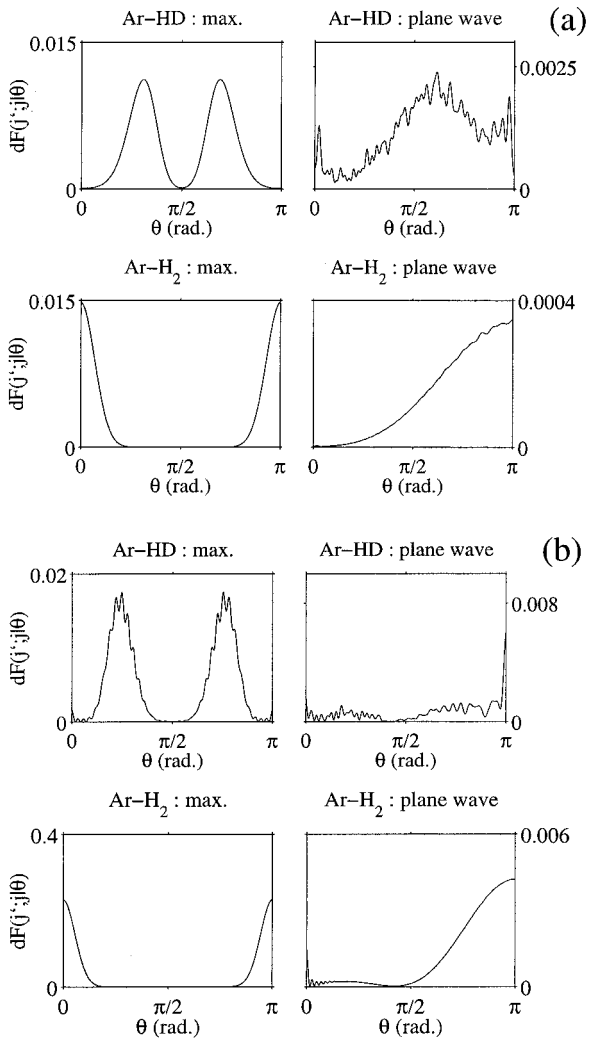

Figure 4. Differential outgoing flux for the case of maximal flux (left) and for a plane-wave (right), for the Ar−HD system (top) and the Ar−H_2 system (bottom). Results are for optimization using the flux-normalization condition: (a) $j' = 4 \leftarrow j = 2$, $m_j = 0$ optimization; (b) $j' = 0 \leftarrow j = 2$, $m_j = 0$ optimization. The plotted flux is a sum over all final $m_{j'}$ values.

5.3. Optimization Constrained by the Normalization of the Incoming Wave. In the second approach, we require that the incoming wavefunction be normalized as

$$\int \mathrm{dR}\mathrm{d}\hat{\mathrm{r}}\psi^{in,(1)*}_{j_1}(\mathrm{R}, \hat{\mathrm{r}})\psi^{in,(2)}_{j_2}(\mathrm{R}, \hat{\mathrm{r}}) = \delta_{j_1 j_2}\delta(k^{(1)}_{j_1} - k^{(2)}_{j_2}) \tag{52}$$

As in eq 45, the coefficients $d^{m_j m_l}_{jl'}$ are given by

$$d^{m_j m_l}_{jl} = i^l \sqrt{\pi}\sqrt{2l+1}e^{i\theta^{m_j 0}_{jl'}}\delta_{m_j m^0}\delta m_{l0} \tag{53}$$

The extrema are obtained at θ values which satisfy the condition

$$\frac{\partial F^{scat}(\theta^{m_j 0}_{j0}, \theta^{m_j 0}_{j1}, ..., \theta^{m_j 0}_{jl}, ...)}{\partial \theta^{m_j 0}_{jl}} = 0 \qquad l = 0, 1, 2, ... \tag{54}$$

Equation 54 leads to a system of nonlinear equations, which may have many solutions, corresponding to local minima/maxima. To find the absolute minimum/maximum with high

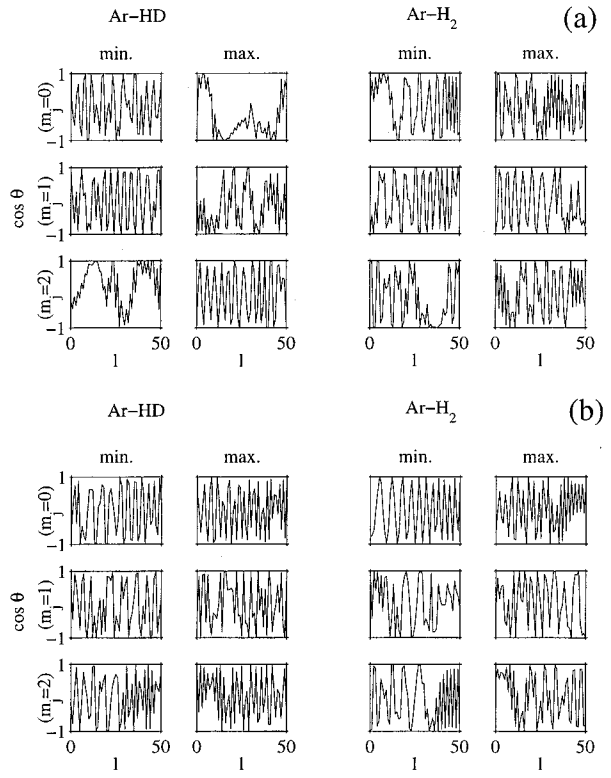

Figure 5. *l*-components of the d_{j,m_j} eigenvector leading to a minimal (left) and a maximal (right) flux for Ar−HD and Ar−H_2: (a) $j' = 4 \leftarrow j = 2$, $m_j = 0$, 1, 2 optimizations; (b) $j' = 4 \leftarrow j = 2$, $m_j = 0$, 1, 2 optimizations. Wavefunction-normalization conditions were used.

probability, we use a simulated annealing algorithm[26] with variables $\theta_{jl}^{m_j 0}$ for $l = 0$ to l_f, where l_f is estimated in section 4.1.

The maximal and minimal fluxes for the $j' = 4 \leftarrow j = 2$, $m_j = 0$ transition are shown in Tables 1 and 2 (columns 4 and 5), along with the fluxes into other final channels. For the case of Ar + HD, for example, the range of results into $j' = 4$ obtained with incoming plane-wave normalization is 0.0139 to 0.0220, compared to the flux associated with an incoming plane-wave of 0.0163. The less-constrained maximization associated with the flux norm yielded the considerably larger value of 0.0553. Note, however, that even though the $j' = 4 \leftarrow j = 2$, $m_j = 0$ flux has been maximized, it often still remains small compared to the elastic scattering ($j = j' = 2$).

The phase $\theta_{jl}^{m_j 0}$ leading to a minimal and to a maximal flux for the $j' = 4 \leftarrow j = 2$, $m_j = 0$, 1, 2 and for the $j' = 0 \leftarrow j = 2$, $m_j = 0$, 1, 2 transitions are shown in Figure 5. They show remarkably little uniformity, reflecting the individuality of each optimization. This case-dependence is also evident in the absolute squares of the incoming eigenfunctions leading to maximum and to minimum scattered fluxes, shown, for Ar + HD, in Figure 6. The corresponding differential fluxes for $m_j = 0$ (summed over all possible $m_{j'}$) are shown in Figure 7. Note the significantly different angular distributions associated with the optimized vs plane-wave results (Figure 4). Analogous results were obtained for Ar + H_2, but space limitations prevent their consideration here.[27]

Additional studies were carried out to assess the stability of the extrema. For example, the phase of each θ contributing to $d_{jl}^{m_j m_l}$ was vaired by π to determine the effect of such changes on the yield. Results showed that the yield was strongly affected by variations in some angles and totally insensitive to changes in others. An alternate study involved random changes in the values of the phases from their values at the extremum, over a range of −0.3 to 0.3 radians. The flux was found to be sensitive to some of these variations, but a wide variety of phases in this range produced similar flux values.

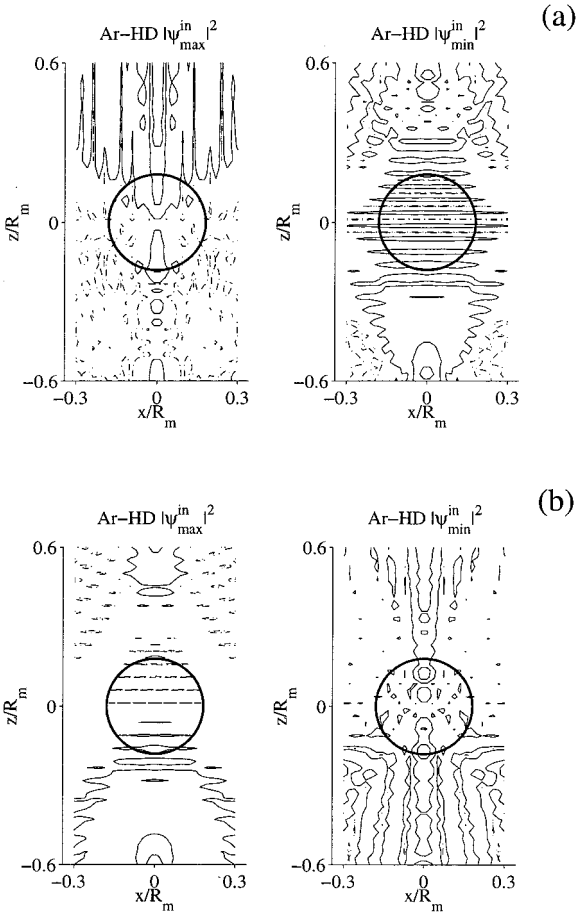

Figure 6. Square of the absolute value of the incoming wavefunctions leading to maximum and minimum outgoing flux for the Ar−HD system using the wavefunction-normalization condition. (a) $j' = 4 \leftarrow j = 2$, $m_j = 0$ optimization, maximum values are 169 for $|\psi_{max}^{in}|^2$ and 138 for $|\psi_{min}^{in}|^2$; (b) $j' = 0 \leftarrow j = 2$, $m_j = 0$ optimization, maximum values are 193 for $|\psi_{max}^{in}|^2$ and 30 for $|\psi_{min}^{in}|^2$. Contour values are as in Figure 3.

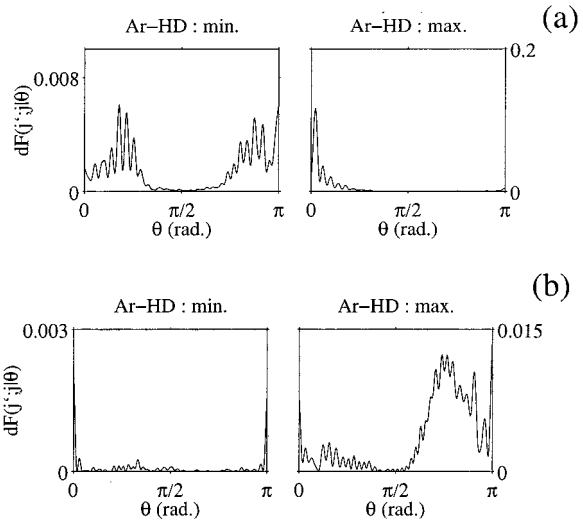

Figure 7. Differential outgoing flux for wavefunctions leading to a minimal flux (left) and a maximal flux (right) for Ar−HD using the wavefunction-normalization condition: (a) $j' = 4 \leftarrow j = 2$, $m_j = 0$ optimization; (b) $j' = 0 \leftarrow j = 2$, $m_j = 0$ optimization.

6. Summary

We have shown that it is possible to significantly alter the nature of the incoming scattering wave in a bimolecular process so as to optimize the scattering into a given product channel. From the viewpoint of coherent control, this is yet another example of how one can superimpose eigenstates in the continuum to produce controllable quantum interferences that affectg the flux into particular channels.

It remains a challenge to produce these modified incoming waves in the laboratory. One possible approach would be to focus the projectile beam or the target beam (or both) with an optical standing wave specifically designed for the purpose.

Acknowledgment. M.S. and P.B. have been greatly influenced through many encounters over the years by the generous spirit of Professor Kent Wilson, a true pioneer in the field of laser chemistry. Support for this research was provided by the U.S. Office of Naval Research, by Photonics Research Ontario, and by the Israel Science Foundation.

Appendix: Orthonormality of General Incoming Waves

In this appendix, we prove the orthogonality properties of (cylindrically asymmetric) incoming waves with arbitrary $d_{jl}^{m_j m_l}$. We also derive the conditions satisfied by $d_{jl}^{m_j m_l}$ when a general incoming wave is constrained to have the normalization of a reference plane-wave.

Orthogonality between plane-waves implies, amongst other things, that two waves propagating along different directions, $\hat{k}^{(1)}$ and $\hat{k}^{(2)}$, are orthogonal to one another. If we insist that the sculpted incoming wavefunctions have this orthogonality property, we must characterize each incoming wavefunction with a $\hat{k}$ vector. However, in contrast to plane-waves, a $\hat{k}$ vector cannot signify the propagation direction of the wavefunction, since a general incoming wavefunctiuon does not have a well-defined propagation direction. The $\hat{k}$ vector should therefore be thought of as a quantum number which helps differentiate one general incoming function from another.

We begin by writing a partial wave expansion, valid over the whole space (and not just in the asymptotic region, as in eq 23), for two incoming wavefunctions, as

$$\psi_{j_1}^{(1)}(\mathrm{R}_1, \hat{\mathrm{r}}) = 2\sum_l \sum_{m_j m_l} d_{jl}^{m_j m_l}\, j_l(k_{j_1}^{(1)} R_1) Y_{lm_l}(\hat{\mathrm{R}}_1) Y_{jm_j}(\hat{\mathrm{r}}) \qquad \text{(A.1)}$$

$$\psi_{j_2}^{(2)}(\mathrm{R}_2, \hat{\mathrm{r}}) = 2\sum_l \sum_{m_j m_l} d_{jl}^{m_j m_l}\, j_l(k_{j_2}^{(2)} R_2) Y_{lm_l}(\hat{\mathrm{R}}_2) Y_{jm_j}(\hat{\mathrm{r}}) \qquad \text{(A.2)}$$

Since in the above expansion, $\hat{\mathrm{R}}_1 \equiv (\theta_1, \phi_1)$ and $\hat{\mathrm{R}}_2 \equiv (\theta_2, \phi_2)$ are expressed relative to the directions of $\boldsymbol{k}_{j_1}^{(1)}$ and $\boldsymbol{k}_{j_2}^{(2)}$, respectively, we first need to express both wavefunctions with respect to the same z axis, which can be chosen as the direction of $\boldsymbol{k}_{j_1}^{(1)}$. Rotating the $\boldsymbol{k}_{j_2}^{(2)}$ vector to coincide with the z axis via three Euler angles (α β, γ), we can write $\psi_j^{(2)}(\mathrm{R}_2, \hat{\mathrm{r}})$ in the common coordinate system as

$$\psi_j^{(2)}(\mathrm{R}_2, \hat{\mathrm{r}}) = 2\sum_l \sum_{m_j m_l} d_{jl}^{m_j m_l} j_l(k_j R) \sum_{m''_l} D_{m_l m''_l}^{(l_2)}(\alpha, \beta, \gamma) Y_{lm''_l}(\hat{\mathrm{R}}_1)(-1)^{m''_l - m_l} Y_{jm_j}(\hat{\mathrm{r}})$$

where $D_{m_l m_l''}^{(l_2)}(\alpha, \beta, \gamma)$ are Wigner rotation matrices.[15] Integration yields

$$\int \mathrm{d}\mathrm{R}_1 \mathrm{d}\hat{\mathrm{r}} \psi_{j_1}^{*(1)}(\mathrm{R}_1, \hat{\mathrm{r}}) \psi_{j_2}^{(2)}(\mathrm{R}_2, \hat{\mathrm{r}}) = 4\sum_{l_1 l_2} \sum_{m_{l_1} m_{l_2} m_{j_1} m_{j_2}} d_{j_1 l_1}^{*m_{j_1} m_{l_1}} d_{j_2 l_2}^{m_{j_2} m_{l_2}} \int R^2 \mathrm{d}R j_{l_1}(k_{j_1}^{(1)} R) j_{l_2}(k_{j_2}^{(2)} R) \times \int \mathrm{d}\hat{\mathrm{R}}\, Y_{l_1 m_{l_1}}^*(\hat{\mathrm{R}}) \sum_{m''_{l_2}} D_{m l_2 m''_{l_2}}^{(l_2)}(\alpha, \beta, \gamma) Y_{l_2 m''_{l_2}}(\hat{\mathrm{R}}) \times (-1)^{m''_{l_2} - m_{l_2}} \int \mathrm{d}\hat{\mathrm{r}}\, Y_{j_1 m_{j_1}}^*(\hat{\mathrm{r}}) Y_{j_2 m_{j_2}}(\hat{\mathrm{r}}) \qquad \text{(A.3)}$$

Using orthonormality relations of the spherical harmonic functions, we obtain

$$\int \mathrm{d}\mathrm{R}_1 \mathrm{d}\hat{\mathrm{r}} \psi_{j_1}^{*(1)}(\mathrm{R}_1, \hat{\mathrm{r}}) \psi_{j_2}^{(2)}(\mathrm{R}_2, \hat{\mathrm{r}}) = 4\sum_l \sum_{m_{l_1} m_{l_2}} \sum_{m_j} d_{j_1 l}^{*m_j m_{l_1}} d_{j_1 l}^{m_j m_{l_2}} \times \int R^2 \mathrm{d}R\, j_l(k_{j_1}^{(1)} R)\, j_l(k j_2^{(2)} R) \times D_{m_{l_1} m_{l_2}}^{(l)}(\alpha, \beta, \gamma)(-1)^{m_{l_1} - m_{l_2}} \delta_{j_1 j_2}$$

After imposing the Bessel functions orthonormality conditions, we obtain

$$\int \mathrm{d}\mathrm{R}_1 \mathrm{d}\hat{\mathrm{r}} \psi_{j_1}^{*(1)}(\mathrm{R}_1, \hat{\mathrm{r}}) \psi_{j_2}^{(2)}(\mathrm{R}_2, \hat{\mathrm{r}}) = 4\sum_l \sum_{m_{l_1} m_{l_2}} \sum_{m_j} \mathrm{d}_{j_1 l}^{*m_j m_{l_1}} \mathrm{d}_{j_1 l}^{m_j m_{l_2}} \times \int R^2 \mathrm{d}R\, j_l(k_{j_1}^{(1)} R)\, j_l(k_{j_2}^{(2)} R) \times D_{m_{l_2} m_{l_1}}^{(l)}(\alpha, \beta, \gamma)(-1)^{m_{l_1} - m_{l_2}} \delta_{j_1 j_2}$$

Therefore, the angular normalization requirement is

$$\delta(\hat{k}_{j_1}^{(1)} - \hat{k}_{j_2}^{(2)}) = \frac{1}{4\pi^2} \sum_l \sum_{m_{l_1} m_{l_2}} \sum_{m_j} d_{j_1 l}^{*m_j m_{l_1}} d_{j_1 l}^{m_j m_{l_2}} D_{m_{l_2} m_{l_1}}^{(l)}(\alpha, \beta, \gamma)(-1)^{m_{l_1} - m_{l_2}}$$

Using the identities

$$\delta(\hat{k}_{j_1}^{(1)} - \hat{k}_{j_2}^{(2)}) = \sum_l \sum_{m_2} Y_{lm_2}^*(\hat{k}_{j_1}^{(1)}) Y_{lm_2}(\hat{k}_{j_2}^{(2)}) \qquad \text{(A.4)}$$

$$Y_{lm}(\hat{k}_{j_2}^{(2)}) = \sum_{m''} D_{mm''}^{(l)}(\alpha, \beta, \gamma) Y_{lm''}(\hat{k}_{j_1}^{(1)})(-1)^{m'' - m} \qquad \text{(A.5)}$$

we obtain

$$\delta(\hat{k}_{j_1}^{(1)} - \hat{k}_{j_2}^{(2)}) = \sum_l \sum_{m_{l_2}} Y_{lm_{l2}}^*(\hat{k}_{j_1}^{(1)}) \sum_{m_{l1}} D_{m_{l2} m_{l1}}^{(l)}(\alpha, \beta, \gamma) Y_{lm_{l1}}(\hat{k}_{j_1}^{(1)})(-1)^{m_{l1} - m_{l2}}$$

$$0 = \sum_l \sum_{m_{l_1}} \sum_{m_{l_2}} \left[\sum_{m_j} \frac{1}{4\pi^2} d_{j_1 l}^{m_j m_{l1}} d_{j_1 l}^{m_j m_{l2}} - Y_{lm_{l1}}(\hat{k}_{j_1}^{(1)}) Y_{lm_{l2}}(\hat{k}_{j_2}^{(2)}) \right] \times D_{m_{l2} m_{l1}}^{(l)}(\alpha, \beta, \gamma)(-1)^{m_{l1} - m_{l2}} \qquad \text{(A.6)}$$

Using the orthogonality and normalization of the rotation matrices (see ref 15, eq 4.6.1)

$$\frac{1}{8\pi^2} \int_0^{2\pi} \int_0^{\pi} \int_0^{2\pi} D_{m'_1 m_1}^{(l_1)}(\alpha, \beta, \gamma) D_{m'_2 m_2}^{(l_2)}(\alpha, \beta, \gamma) \mathrm{d}\alpha \sin\beta d\beta d\gamma = \delta_{m'_1 m_1} \delta_{m'_2 m_2} \delta_{l_1 l_2} \frac{1}{2l_1 + 1} \qquad \text{(A.7)}$$

we obtain, my multiplying eq A.6 by $D_{m'_{l2} m'_{l1}}^{(l')}(\alpha, \beta, \gamma)$ and integrating,

$$0 = \sum_{m_j} \frac{1}{4\pi^2} d^{*m_j m_{l1}}_{j_1 l} d^{m_j m_{l2}}_{j_1 l} - Y_{lm_{l1}}(\hat{k}^{(1)}_{j_1}) Y_{lm_{l2}}(\hat{k}^{(2)}_{j_2}) \quad \text{(A.8)}$$

Finally, choosing $\hat{k}^{(1)}_{j_1} = (0, 0)$, we obtain the normalization condition on the $d^{m_j m_l}_{jl}$ coefficients as

$$\sum_{m_j} d^{*m_j m_{l1}}_{j_1 l} d^{m_j m_{l2}}_{j_1 l} = \pi(2l+1)\delta_{m_{l1}0}\delta_{m_{l2}0} \quad \text{(A.9)}$$

for every l, m_{l_1}, and m_{l_2}.

References and Notes

(1) For recent reviews, see: Shapiro, M.; Brumer, P. *J. Chem. Soc., Faraday Trans. 2* **1997**, *93*, 1263. Gordon, R. J.; Rice, S. A. *Annu. Rev. Phys. Chem.* **1997**, *48*, 595.

(2) Brumer, P.; Shapiro, M. *Sci. Am.* **1995**, *272*, 56.

(3) Shapiro, M.; Brumer, P. *Phys. Rev. Lett.* **1996**, *77*, 2574. Holmes, D.; Shapiro, M.; Brumer, P. *J. Chem. Phys.* **1996**, *105*, 9162.

(4) Abrashkevich, A. G.; Shapiro, M.; Brumer, P. *Phys. Rev. Lett.* **1998**, *81*, 3789. Errata: *Phys. Rev. Lett.* **1999**, *82*, 3002.

(5) Frishman, E.; Shapiro, M.; Brumer, P. *J. Chem. Phys.* **1999**, *110*, 9.

(6) Brumer, P.; Abrashkevich, A. G., Shapiro, M. *Far. Discuss. Chem. Soc.*, in press.

(7) Tannor, D. J.; Rice, S. A. *Adv. Chem. Phys.* **1988**, *70*, 441. Tannor, D. J.; Rice, S. A. *J. Chem. Phys.* **1985**, *83*, 5013. Tannor, D. J.; Kosloff, R.; Rice, S. A. *J. Chem. Phys.* **1986**, *85*, 5805.

(8) Seideman, T.; Shapiro, M.; Brumer, P. *J. Chem. Phys.* **1989**, *90*, 7132.

(9) Yan, Y.; Gillilan, R. E.; Whitnell, R. M.; Wilson, K. R. *J. Phys. Chem.* **1993**, *97*, 2320. Krause, J. L.; Whitnell, R. M.; Wilson, K. R.; Yan, Y.; Mukamel, S. *J. Chem. Phys.* **1993**, *99*, 6562.

(10) Warren, W. S.; Rabitz, H.; Dahleh, M. *Science* **1993**, *259*, 1581.

(11) Bardeen, C. J.; Yakovlev, V. V.; Wilson, K. R.; Carpenter, S. D.; Weber, P. M.; Warren, W. S. *Chem. Phys. Lett.* **1997**, *280*, 151.

(12) Assion, T.; Baumert, T.; Bergt, M.; Brixner, T.; Kiefer, B.; Seyfried, V.; Strehle, M.; Ferber, G. *Science* **1988**, *282*, 919.

(13) Arthurs, A. M.; Dalgarno, A. *Proc. R. Soc. London* **1960**, *256*, 540.

(14) *Atom−Molecule Collision Theory*; Bernstein, R. B., Ed.; Plenum Press: New York, 1979; Chapters 6, 8, 9, 10.

(15) Edmonds, A. R. *Angular Momentum in Quantum Mechanics*; Princeton University Press: Princeton, NJ, 1960; Chapter 3 (Section 5, eqs 3, 4, and 16).

(16) Johnson, B. R.; Secrest, D.; Lester, W. A.; Bernstein, R. B. *Chem. Phys. Lett.* **1967**, *1*, 396.

(17) Lester, W. A.; Bernstein, R. B. *Chem. Phys. Lett.* **1967**, *1*, 207.

(18) Dewangan, D. P.; Flower, D. R. *J. Phys. B* **1981**, *14*, 2179.

(19) Sun, Y.; Yudson, R. S.; Kouri, D. J. *J. Chem. Phys.* **1989**, *90*, 241.

(20) Bernstein, R. B.; Dalgarno, A.; Massey, H.; Percival, I. C. *Proc. R. Soc. London*, **1963**, *274A*, 427.

(21) Kreek, H.; Le Roy, R. J. *J. Chem. Phys.* **1975**, *63*, 338.

(22) Chu, S. I.; Datta, K. *J. Chem. Phys.* **1982**, *76*, 5307.

(23) Le Roy, R. J.; van Kranendonk, J. *J. Chem. Phys.* **1974**, *61*, 4750.

(24) Herzberg, G.; Huber, K. P. *Molecular Spectra and Molecular Structure*, Part IV; Van Nostrand: New York, 1979.

(25) Gordon, R. G. *J. Chem. Phys.* **1969**, *51*, 14.

(26) (a) Corana, A.; Marchesi, M.; Martini, C.; Ridella, S. *ACM Transactions on Mathematical Software* **1987**, *13*, 262. (b) Goffe, W. L.; Ferrier, G. D.; Rogers, J. *Journal of Econometrics* **1994**, *60*, 65. Fortran source code by Goffe, W. L.

(27) Frishman, E. To appear in Ph.D. dissertation, Weizmann Institute of Science, Rehovot, Israel.